CHEMISTRY
A European Journal

Supporting Information

Design of 2D Porous Coordination Polymers Based on Metallacrown Units

Corrado Atzeri,[a] Luciano Marchiò,[a] Chun Y. Chow,[b] Jeff W. Kampf,[b] Vincent L. Pecoraro,*[b] and Matteo Tegoni*[a]

chem_201600562_sm_miscellaneous_information.pdf

Table of Contents

EXPERIMENTAL SECTION

X-ray Crystal Determination. Crystals of dimensions 0.23 × 0.23 × 0.16 mm of **1**, or crystals of dimensions 0.10 × 0.10 × 0.02 mm of **2** were mounted on a Rigaku Saturn944+ CCD-based X-ray diffractometer equipped with a low-temperature device and fine-focus Cu-target X-ray tube (λ = 1.54187 Å). The X-ray intensities were measured at 85(2) K; A total of 107642 and 80642 reflections were collected for **1** and **2**, respectively. The frames were integrated with the CrystalClear-SM Expert 2.0 Rigaku software package.[1] The structures were solved and refined with the Bruker SHELXTL (version 2008/3) software package.[2] In **1**, the data collection was considerably affected by the poor crystal quality, and several restraints were used to model the hydroxamate moieties. The pyridine ring bound to the central metal was found disordered in two positions. The pyridine and acetate moieties of the peripheral copper atom were also statically disordered over two sites. The disordered fragments were refined with isotropic thermal parameters. The residual electron density found into the structural cavities was treated with the SQUEEZE program.[3] In **2**, on one of the metal centers a DMSO/pyridine moiety was found disordered. These coordinated molecules were refined with site occupancy factors (s.o.f.) of 0.7 (DMSO) and 0.3 (pyridine). In the lattice, solvent of crystallization was present and it could be tentatively located from the difference Fourier map as pyridine and DMSO molecules. The hydrogen atoms placed in idealized positions. Additional details are presented in Table S1 and are given as supporting information in a CIF file.

Materials and methods: all reagents and solvents were obtained from commercially available sources and were used without further purification. Inert atmosphere was achieved in N_2 using Schlenk techniques. Flash column chromatography was performed using silica gel (230-400 mesh) from Sigma-Aldrich. ^{1}H and ^{13}C NMR spectra were recorded on Varian MR400 and Vnmrs500 spectrometers using standard pulse sequences. Chemical shifts were referenced to residual solvent protons. Infrared spectra were recorded on a Perkin-Elmer FTIR Nexus spectrometer using a Smart Orbit HATR accessory equipped with a diamond crystal. Electrospray

ionization mass spectra (ESI-MS) were collected on a Micromass LCT TOF electrospray ionization mass spectrometer. Capillary voltage 3.0 V and negative cone voltage of -40 V (ESI- ion mode) were used. Desolvation temperatures were set at 150 °C for methanolic solutions, and 200 °C for solutions in DMF. Samples (40 μM) were injected through direct infusion using a syringe pump at 10 μl/min, and the spectra recorded in full scan analysis mode in the range 100-2000 m/z. Elemental analysis (C, H, N) were performed by Atlantic Microlab, Inc. (Atlanta, GA, United States). Thermogravimetric analysis was performed on a Perkin-Elmer TGA-7 thermogravimetric analyzer using a temperature ramp rate of 5 °C/min from 50 to 700 °C, under a N_2 flow of 20.0 mL/min. Differential scanning calorimetry was performed on a Perkin-Elmer DSC-6000 analyzer equipped with Intracooler, with a temperature ramp rate of 5 °C/min from 20.0 °C to either 200 or 400°C, under a N_2 flow of mL/min.

The synthesis of hinHA was modified from a previously reported route for the synthesis of hydroxamic acids.[4]

Synthesis of *N*-(benzyloxy)-3-hydroxyisonicotinamide (BzOhinHA): 3-hydroxy-4-pyridinecarboxylic acid (5.42 g, 38.99 mmol) and *N,N*-diisopropylethylamine (13.58 mL, 77.98 mmol) were mixed in dry CH_2Cl_2 (150 mL) in a two-necked round bottom flask under nitrogen atmosphere. Solid carbonyldiimidazole (6.64 g, 40.94 mmol) was added and the solution was kept stirring under nitrogen atmosphere for 3h at room temperature. Solid *O*-benzylhydroxylamine hydrochloride (6.53 g, 40.94 mmol) was added and the solution heated under reflux for 8 hours under stirring. The solvent was evaporated *in vacuo* yielding a dark red oil, which was diluted with distilled water (10 mL). The solution was acidified to pH = 5 with a solution of acetic acid (5 M), and left at 4 °C overnight. The pink precipitate was filtered, washed with of cold water (5 mL), and dried uder vacuum. The product was purified through silica column chromatography using CH_2Cl_2/MeOH 95/5 as the eluent. The pure product was isolated as a yellow powder (6.45 g, 68%). ^{1}H NMR (500 MHz, [D_4]MeOH) δ: 8.20 (s, 1H), 8.04 (d, J = 5.2 Hz, 1H), 7.72 (d, J = 5.2 Hz, 1H), 7.52 – 7.46 (m, 2H), 7.44 – 7.33 (m, 3H), 4.87 (s, 3H). IR (cm^{-1}): 3086w, 3025w, 2926w, 2860w, 1634m, 1579m, 1524m, 1493m, 1454m,

1438m, 1377m, 1352m, 1310s, 1237m, 1218m, 1203m, 1160m, 1139w, 1096w, 1080w, 1004s, 916m, 870m, 830s, 781s, 754s, 699s, 683s. Anal. calc. for $C_{14}H_{13}N_2O_3$: C, 63.93; H, 4.95; N, 11.47; found: C, 63.8; H, 4.9; N, 11.5%. ESI+: *m/z* calc. for [M - H^+] = 243.1; found = 243.0.

Synthesis of 3-hydroxyisonicotine hydroxamic acid (hinHA): *N*-(benzyloxy)-3-hydroxyisonicotinamide (1.00 g, 4.09 mmol) was dissolved in CH_2Cl_2 (5 mL), diluted with of degassed MeOH (350 mL), and hydrogenated in the presence of Pd/C (10%, 200 mg) under $H_{2(g)}$ (p_{H2} = 1 atm) for 24 hours. The product precipitated out, and it was separated from the catalyst by washing the solid with hot methanol (200 mL). The solvent was removed *in vacuo* and the product purified by recrystallization in 2:1 acetone:methanol (8 mL), affording a white precipitate (0.50 g, 80%). ^{1}H NMR (400 MHz, [D_2]water) δ: 7.60 (s, 1H), 7.36 (d, J = 5.1 Hz, 1H), 7.20 (d, J = 5.1 Hz, 1H). IR (cm^{-1}): 3126w, 3080w, 2572s(br), 2111m, 1646s, 1619s, 1591m, 1506s, 1444s, 1380s, 1310m, 1252s, 1182s, 1154m, 1080m, 1050m, 1016s, 959m, 901s, 870s, 836m,818s, 769s, 705m, 638s, 583s, 573s, 543s. Anal. calc. for $C_6H_6N_2O_3$: C, 46.76; H, 3.92; N, 18.18; found: C, 46.8; H, 4.0; N, 18.0%. ESI- (negative ion mode): *m/z* calc. for [M - H^+] = 153.0; found = 153.0.

Synthesis of network $\{[Cu(II)(AcO)Py]_2\{Cu(II)[12\text{-}MC_{Cu(II),\ hinHA}\text{-}4]\}\}_n$ (1): The ligand hinHA (20 mg, 0.13 mmol, 4 eq.) was dissolved in a 2:1 DMF:pyridine (20:10 mL) mixture. A solution of copper(II) acetate monohydrate (45 mg, 0.23 mmol, 7 eq.) in 2:1 DMF:pyridine (20:10 mL) was added under stirring. The mixture immediately turned green, due to the formation of the 12-MC-4 species. After 30 minutes under stirring, the suspension was filtered to remove insoluble impurities, and the product left to crystallize by slow evaporation into test tubes in a fume hood. Green rods suitable for single-crystal X ray diffraction were obtained over the course of two weeks. IR (cm^{-1}): 3284w(br), 1652m, 1564s, 1487m, 1420s, 1380s, 1331s, 1236s, 1191m, 1111w, 1072m, 1026s, 959s, 888m, 815m, 702s, 680s, 656s, 607s. ESI-MS (on mother solution): *m/z* calc. for $\{Cu(II)[12\text{-}MC_{Cu(II),\ hinHA}\text{-}4]\}^{2-}$ = 460, found = 460; *m/z* calc. for $[\{Cu(II)[12\text{-}MC_{Cu(II),\ hinHA}\text{-}4]\}^{2-} + Na^+]^-$ = 943, found = 943.

Synthesis of $\{(NEt_4)_2\{Cu(II)[12\text{-}MC_{Cu(II),\ hinHA}\text{-}4](DMSO)_{1.4}(Py)_{0.6}\}(DMSO)_{0.4}(Py)_{0.6}\}_n$ (2): ligand hinHA (40 mg, 0.26 mmol, 4 eq.) was dissolved in a 3:2:1 DMSO:DMF:pyridine solution (6 mL). Solid tetraethylammonium acetate (204 mg, 0.78 mmol, 12 eq.) and copper(II) triflate (106 mg, 0.32 mmol, 1.25 eq.) were added under stirring. Insoluble impurities were removed by filtration and the solution was left in a closed vessel at 0 °C yielding green crystalline plates of the product over the course of three weeks. Crystals have low stability out of the mother liquors. X-ray diffraction data were collected at low temperature. ESI-MS: *m/z* calc. for $\{Cu(II)[12\text{-}MC_{Cu(II),\ hinHA}\text{-}4]\}^{2-}$ = 460, found = 460.

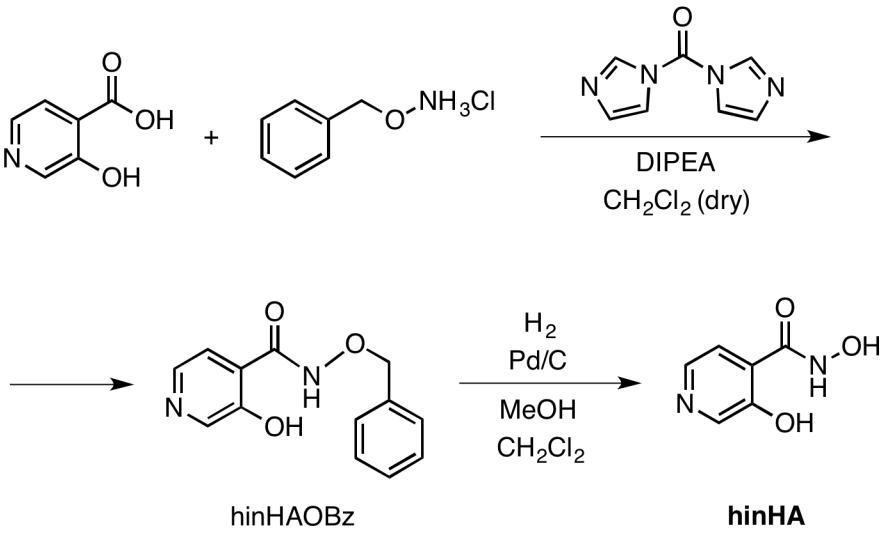

Fig. S1: Synthetic route followed for the obtainment of ligand hinHA.

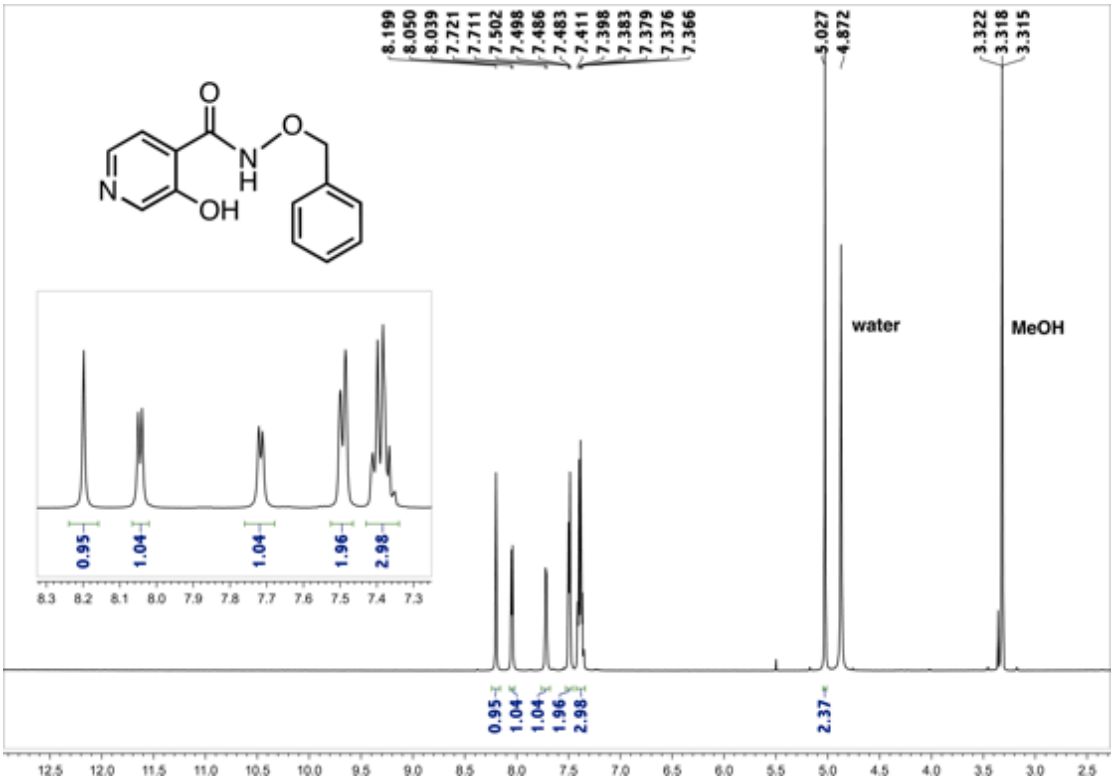

Fig. S2: ^{1}H NMR spectrum of *N*-(benzyloxy)-3-hydroxyisonicotinamide (BzOhinHA) in CD_3OD.

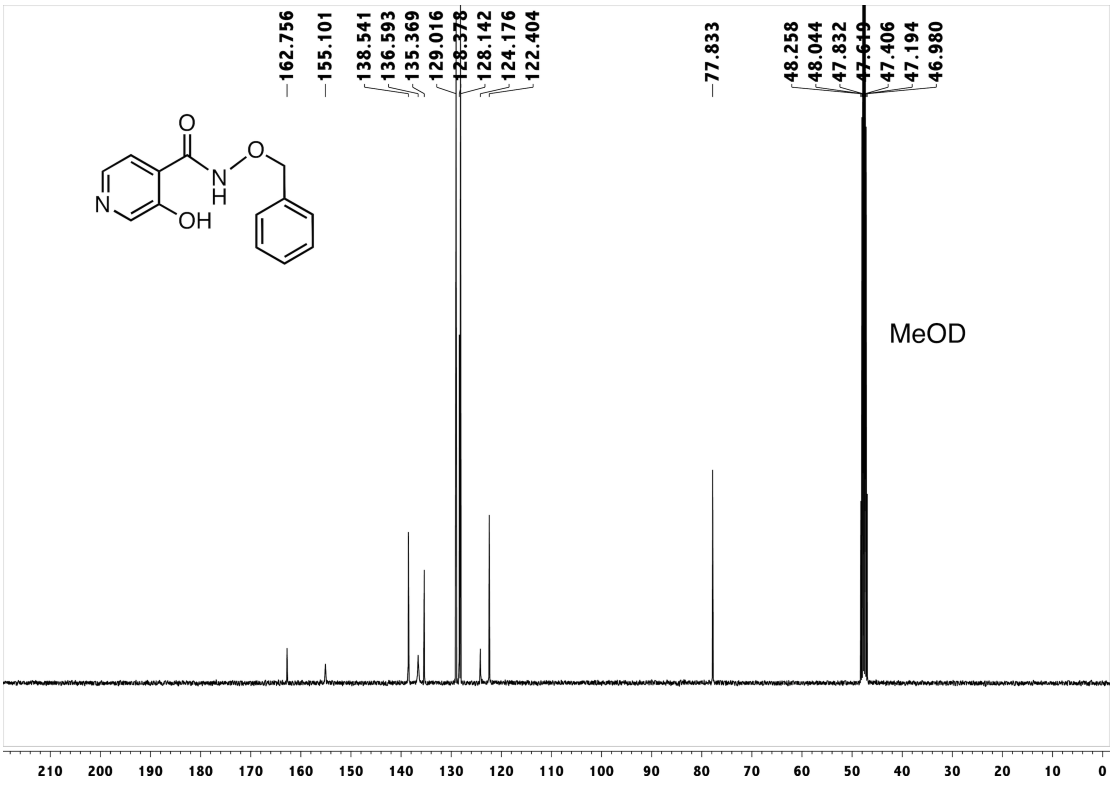

Fig. S3: ^{13}C NMR spectrum of *N*-(benzyloxy)-3-hydroxyisonicotinamide (BzOhinHA) in CD_3OD.

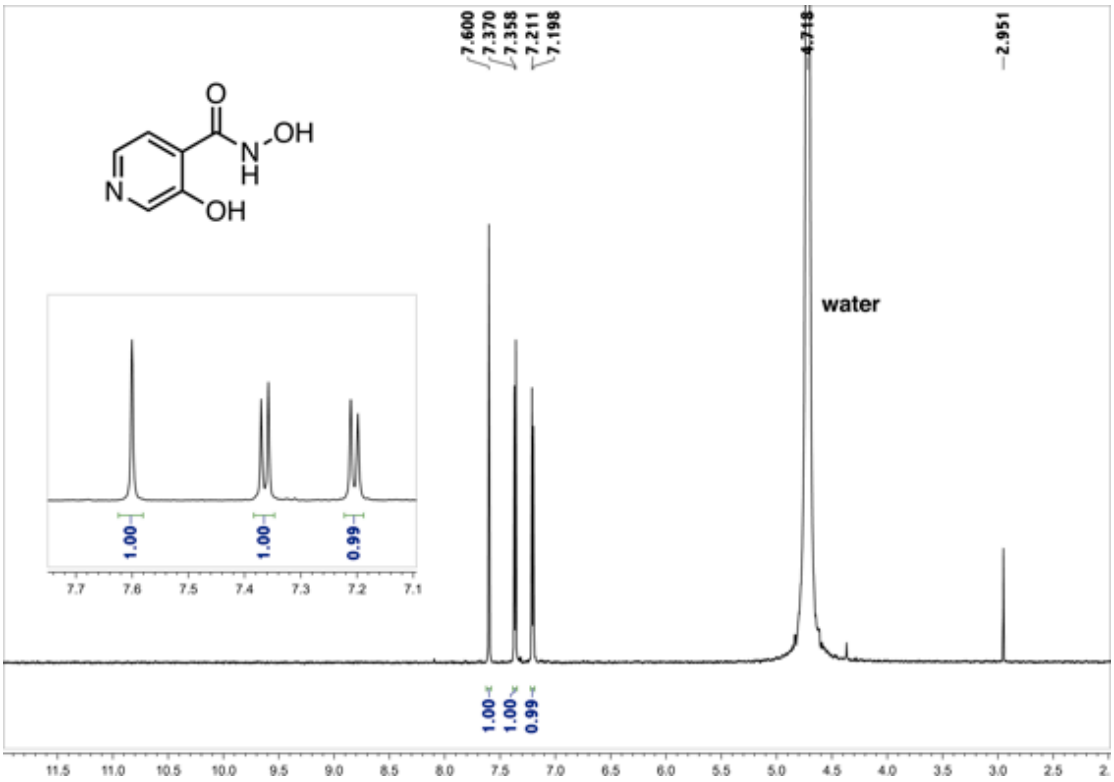

Fig. S4: ^{1}H NMR spectrum of 3-hydroxyisonicotine hydroxamic acid (hinHA) in D_2O.

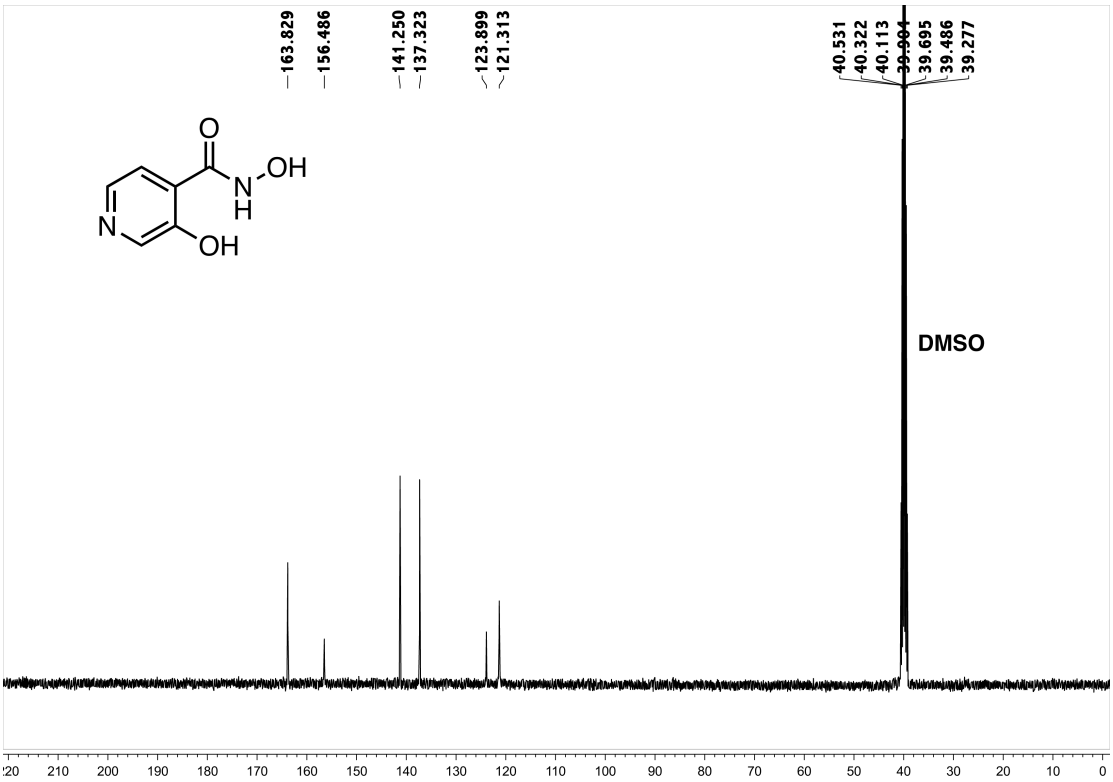

Fig. S5: ^{13}C NMR spectrum of 3-hydroxyisonicotine hydroxamic acid (hinHA) in d_6-DMSO.

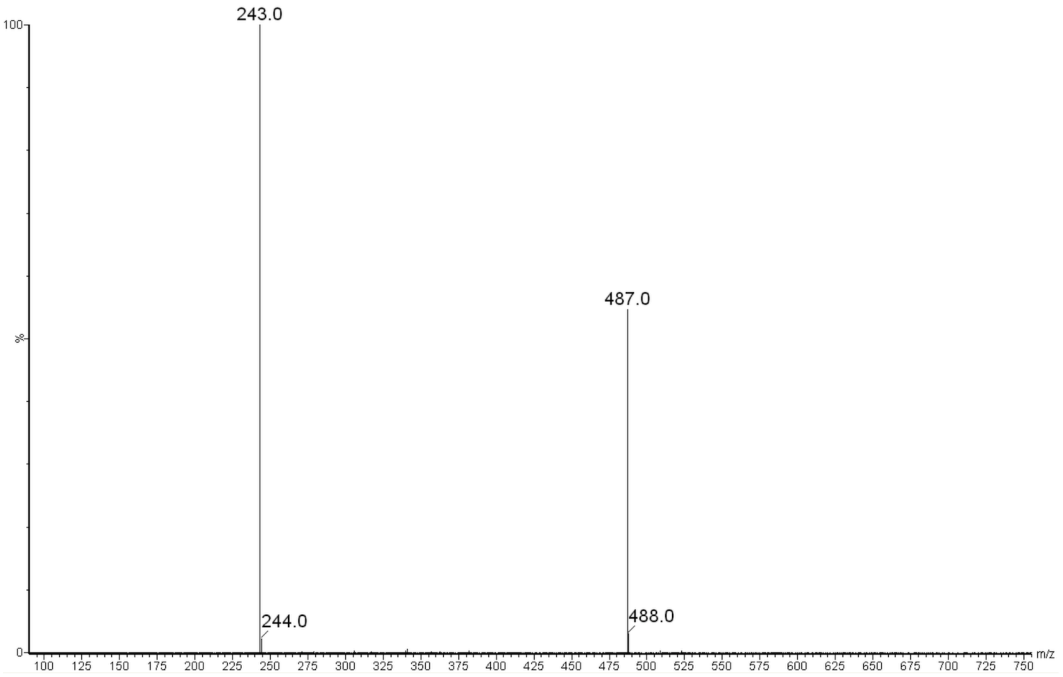

Fig. S6: Negative-ion ESI-MS spectrum of BzOhinHA (M). {M - $1H^+$}: *m/z* 243; {M_2 - $1H^+$}: *m/z* 487.

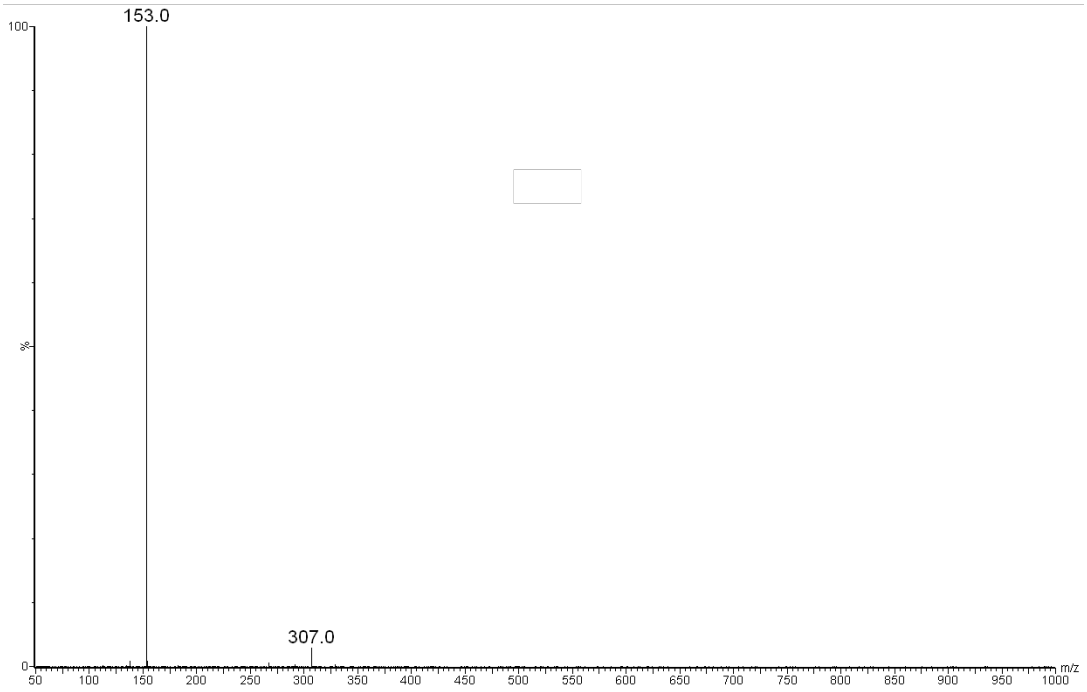

Fig. S7: Negative-ion ESI-MS spectrum of hinHA. (M). {M - $1H^+$}: *m/z* 153; {M_2 - $1H^+$}: *m/z* 307.

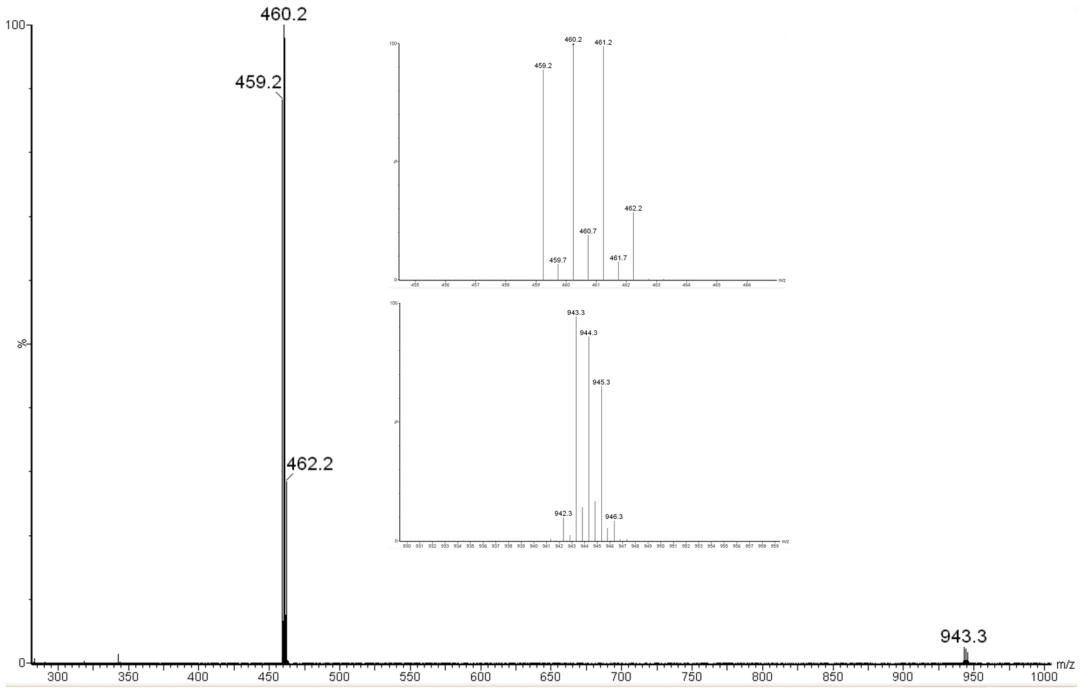

Fig. S8: Negative-ion ESI-MS spectrum of **1.** $\{Cu(II)[12\text{-}MC_{Cu(II),\ hinHA}\text{-}4]\}^{2-}$: *m/z* 460; $Na\{Cu(II)[12\text{-}MC_{Cu(II),\ hinHA}\text{-}4]\}^{-}$: 943 *m/z*. The observed isotopic distribution of the signals is reported in the insect.

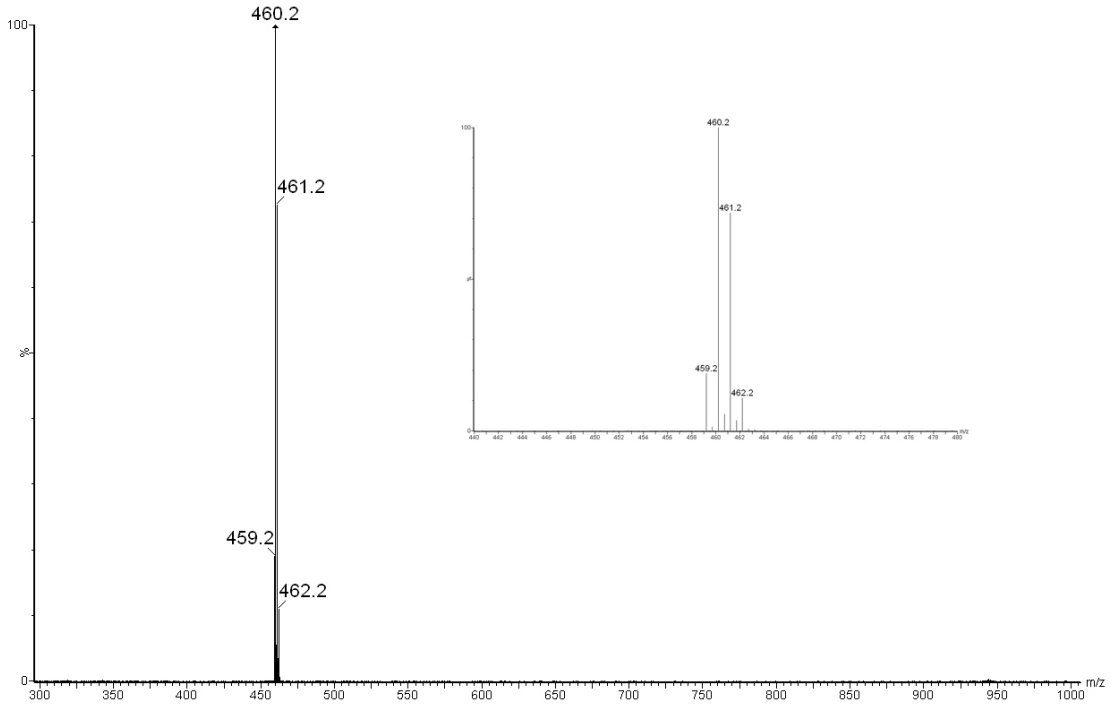

Fig. S9: Negative-ion ESI-MS spectrum of **2.** $\{Cu(II)[12\text{-}MC_{Cu(II),\ hinHA}\text{-}4]\}^{2-}$: *m/z* 460. The observed isotopic distribution of the signal is reported in the insect.

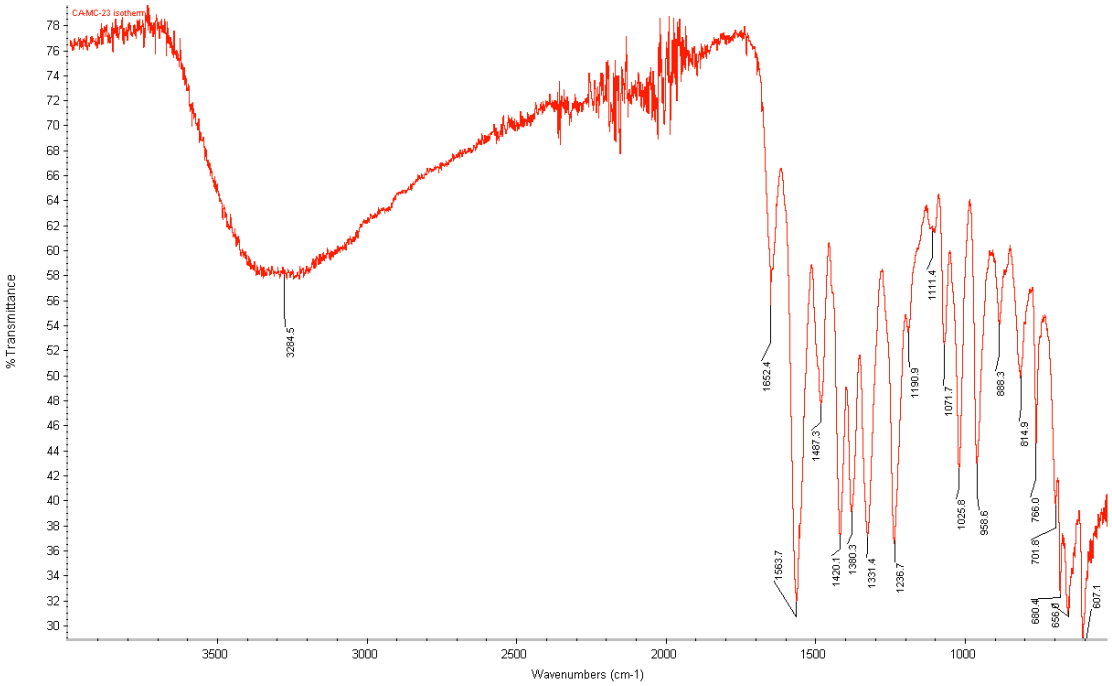

Fig. S10: FT-IR spectrum of **1.**

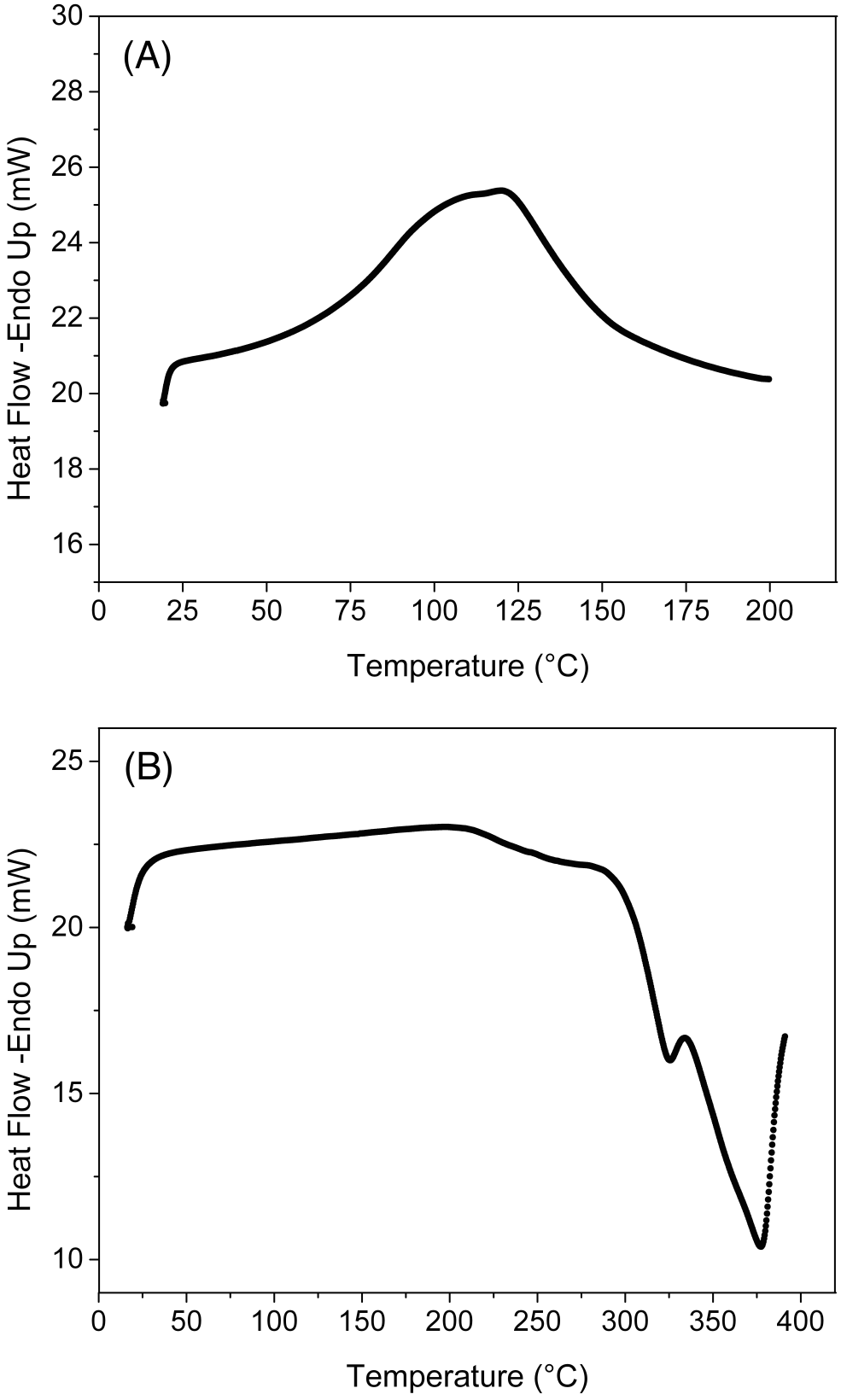

Fig. S11: Differential Scanning Calorimetry analysis on a 24 h air-dried sample of crystals of **1**. Loss of crystallization solvent is evidenced around 110 °C during a first run (A), while subsequent two-step decomposition of the material occurred above 300 °C during a second run (B).

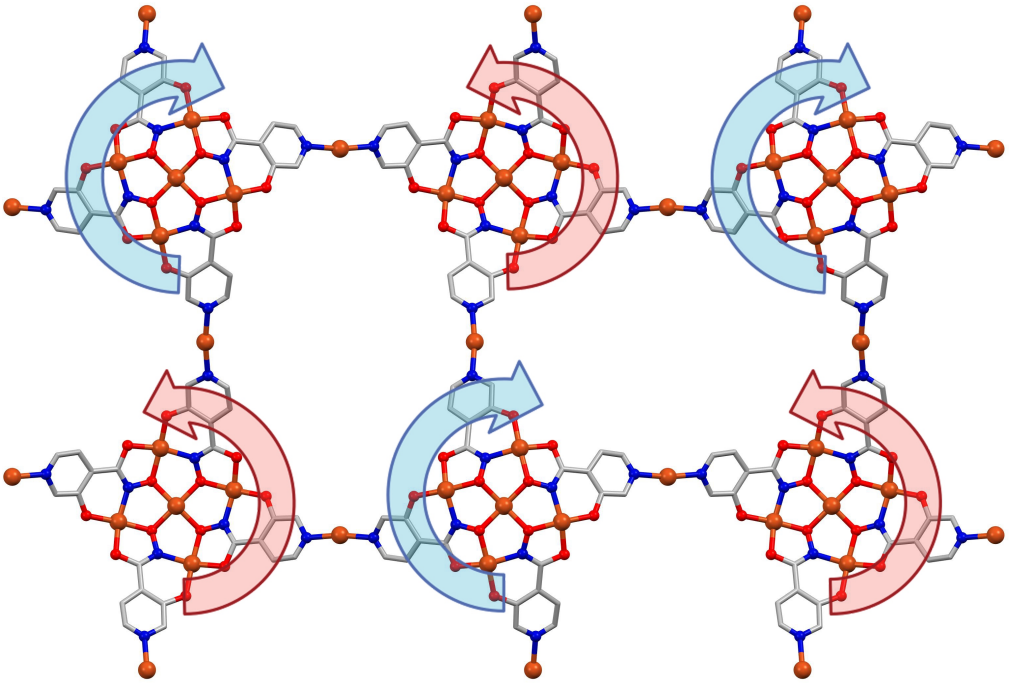

Fig. S12: Representation of the 2D layer of metallacrowns composing network **1**. Clockwise (blue) or anticlockwise (red) rotation of the Cu-O-N connectivity is displayed. The *up-down* alternated repetition of the same bowl-shaped isomer provides network **1** with homochirality. Color scheme: Cu(II), orange; N, blue; O, red; C, grey; H, white.

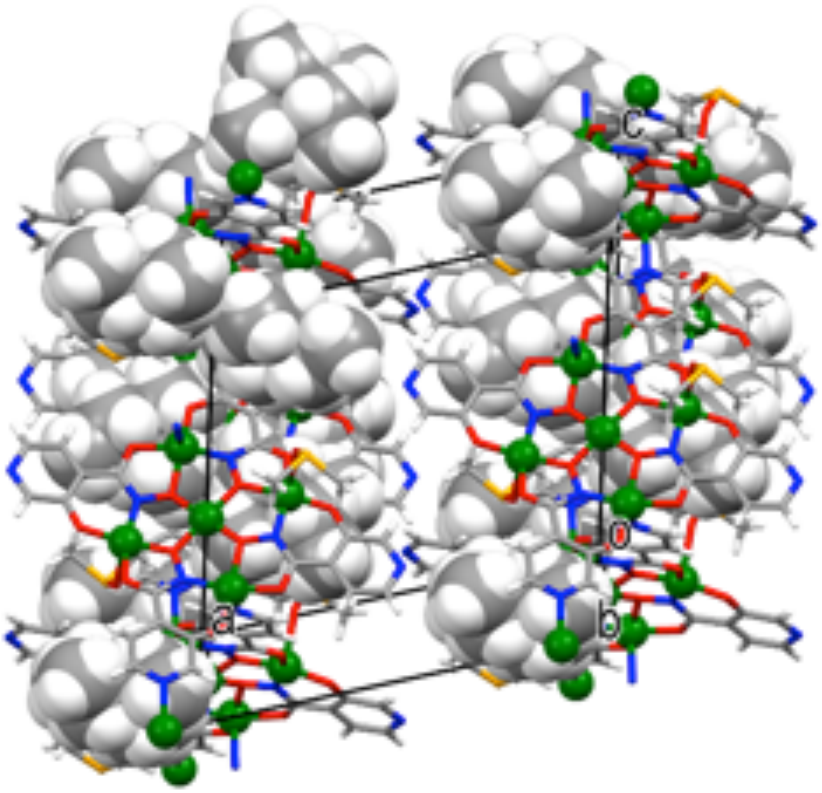

Fig. S13: Depiction of the reticular framework originated by the interacting MCs in **2** as viewed along the *b* axis. The interacting MC platforms are arranged nearly perpendicularly to each other forming a polymeric MC grid hosting Et_4N^+ cations (in spacefill representation). The grids are arranged in layers that are parallel to the *bc* crystallographic plane. The solvent of crystallization (pyridine and DMSO, not shown) is located in the interstices formed by the approaching layers.

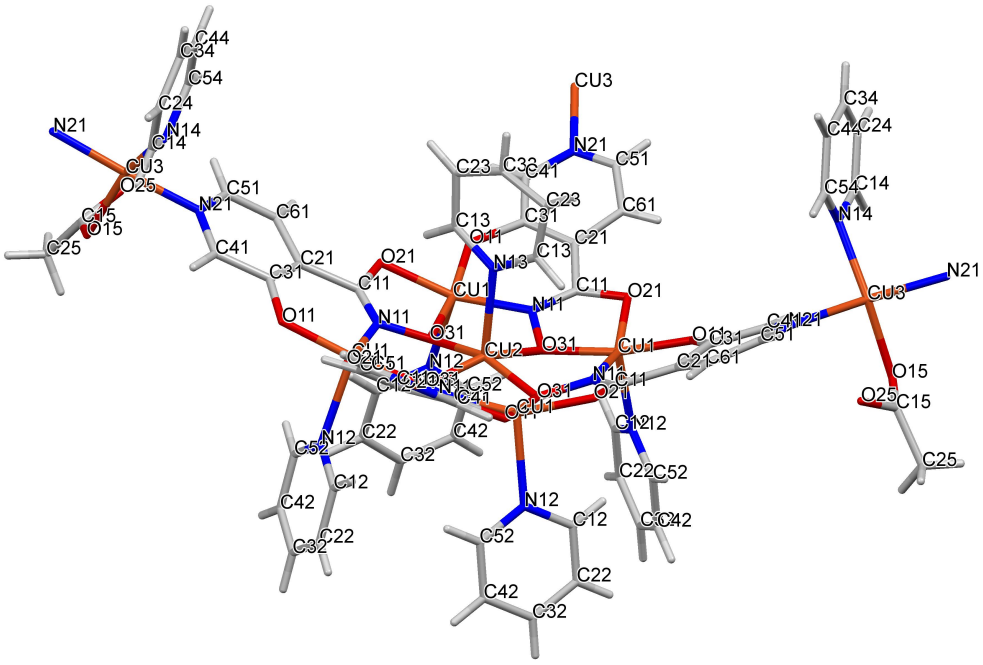

Fig. S14: Structural representation of **1**.

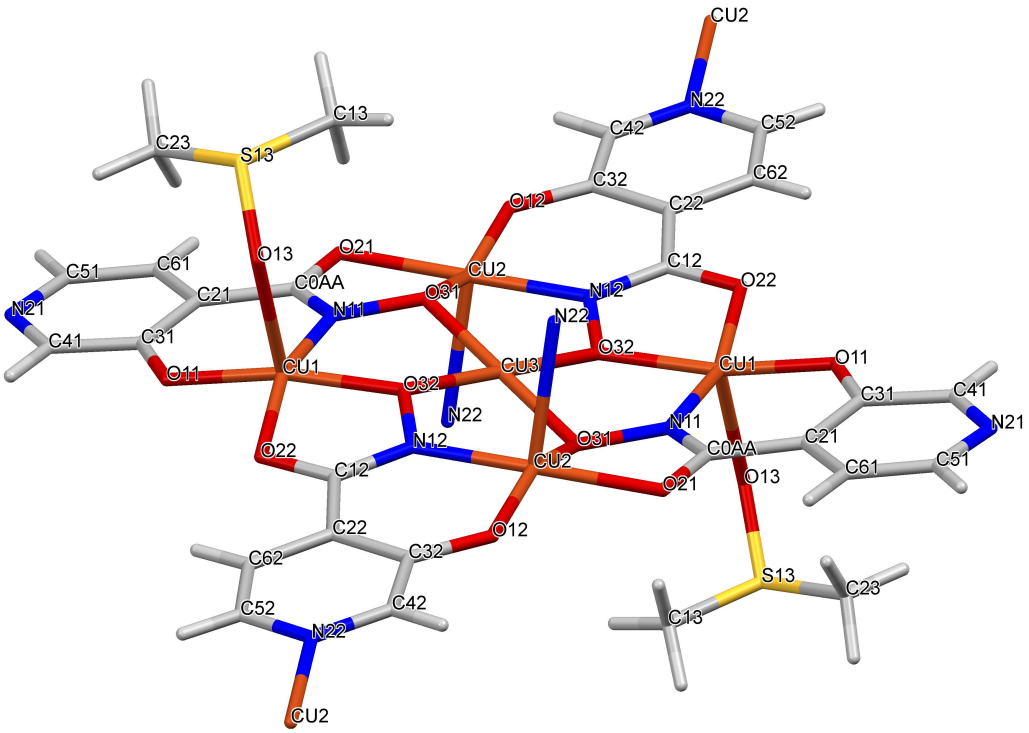

Fig. S15: Structural representation of **2**. Tetraethylammonium counterions (TEA) are not shown.

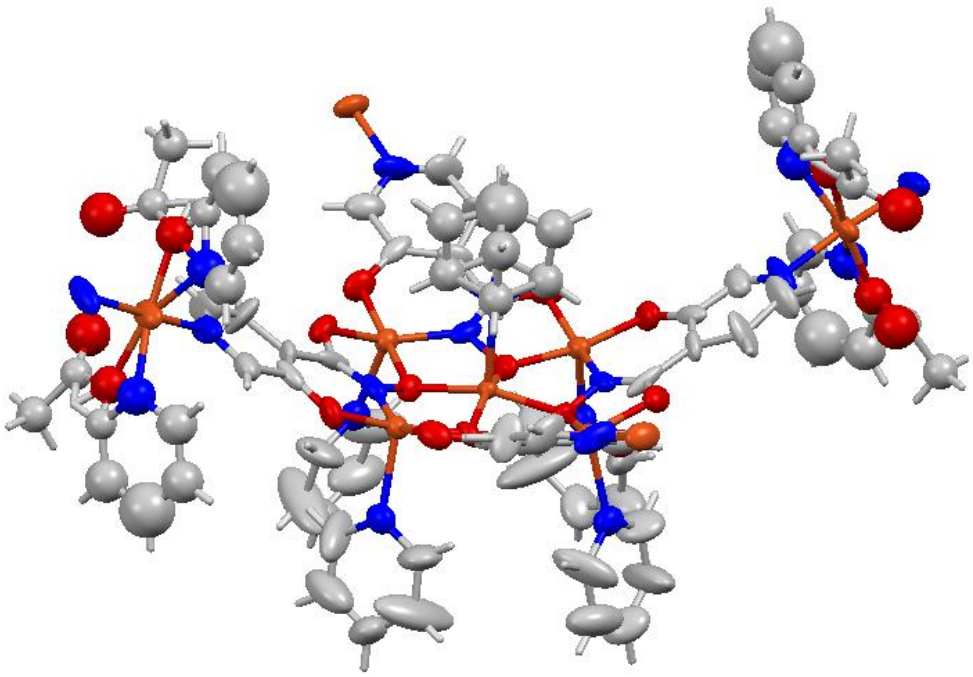

Fig. S16: Ortep representation (ellipsoids at 30% probability level) of **1**. The pyridine and the acetate ions coordinated to the bridging Cu(II) ions are statically disordered in two positions.

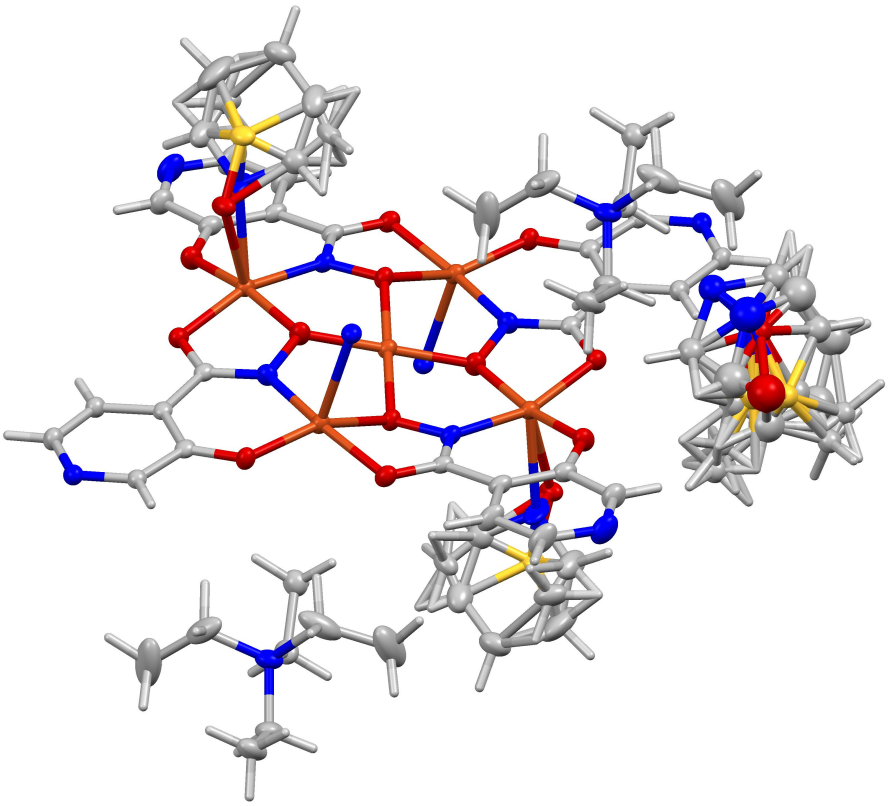

Fig. S17: Ortep representation (ellipsoids at 30% probability level) of **2**. The axial positions of the copper ions are occupied by DMSO (0.7 occupancy *per* site) or pyridine (0.3 occupancy *per* site). The voids in the packing are occupied by pyridine (0.6 molecules) or DMSO (0.4 molecules). The final formula results $\{(NEt_4)_2\{Cu(II)[12\text{-}MC_{Cu(II),\ hinHA}\text{-}4](DMSO)_{1.4}(Py)_{0.6}\}(DMSO)_{0.4}(Py)_{0.6}\}_n$.

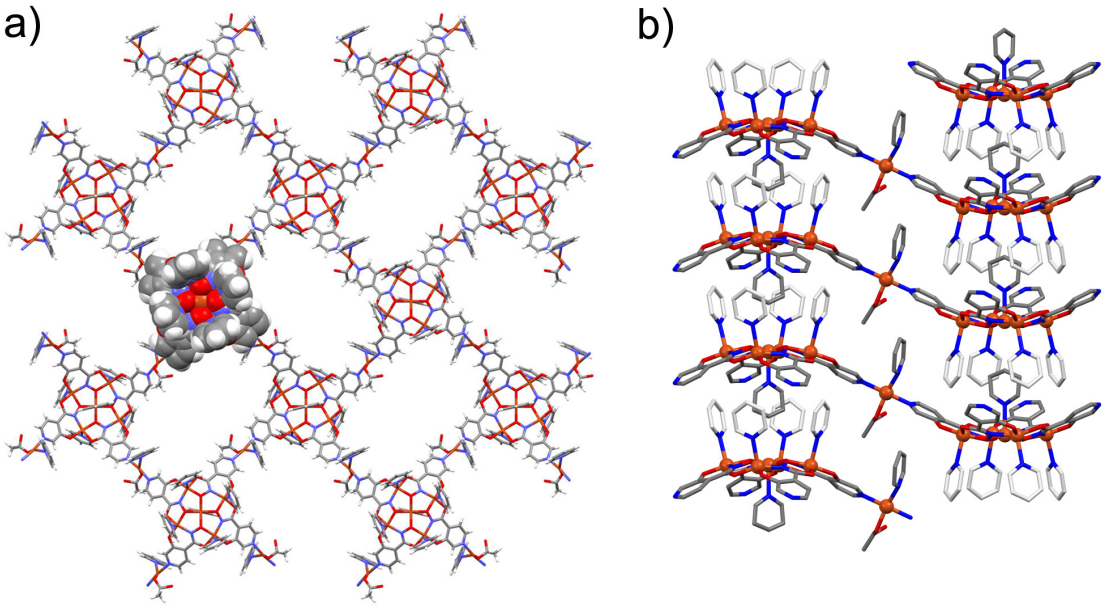

Fig. S18: a) Representation of one layer of the porous network, viewed along the c-axis. One MC unit is shown in a space filling representation. Taking into consideration Van der Waals radii, the 2D pore section measures 12.6 x 8.9 $Å^2$, accounting for 36% of the total cell volume; b) Encapsulation of a coordinated pyridine molecule within the hydrophobic pyridinic pocket forms π-π pillars holding the layers together. Colour scheme: Cu - orange, O - red, N - blue, C - grey, H - white.

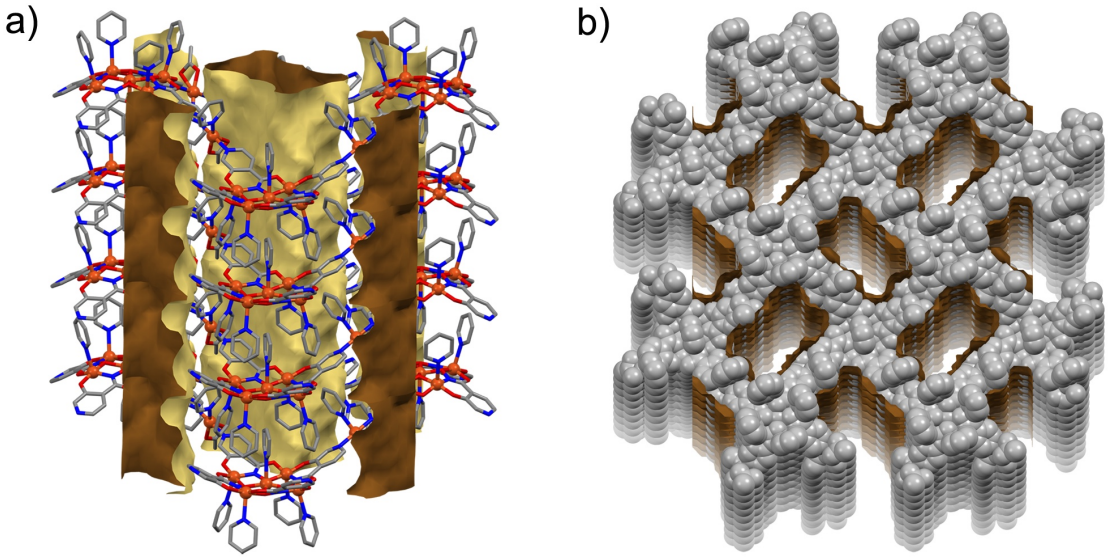

Fig. S19: a) Ball and stick representation of a single MC unit showing the peripheral Cu^{II} ions acting as linkers between the units, viewed along the *c* crystallographic axis; b) Stacking between two MC units forming a pillar parallel to the *c* axis. Colour scheme: Cu - orange, O - red, N - blue, C - grey.

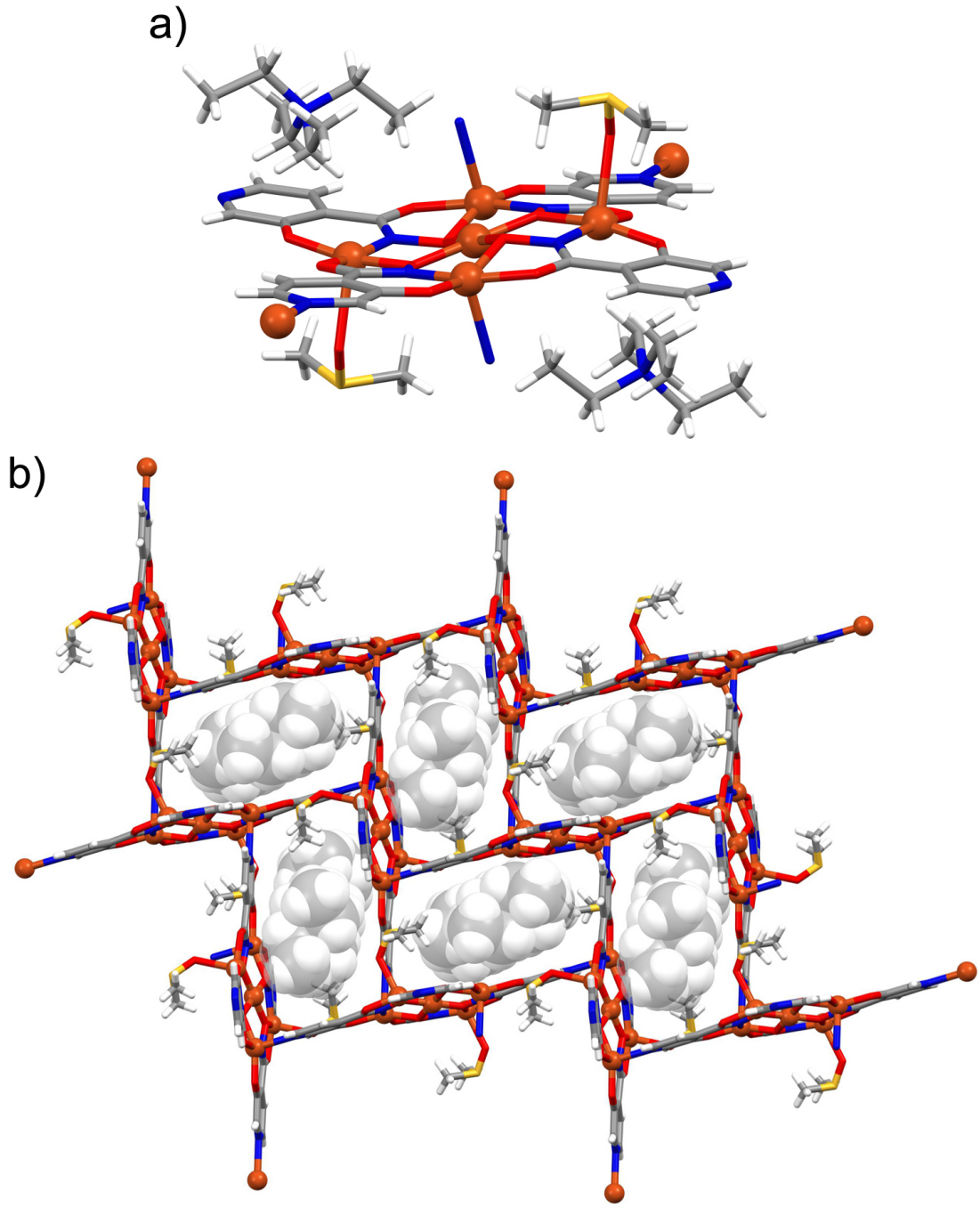

Fig. S20: Structure of **2**, viewed along *a.* a) Single MC unit, with two coordinated DMSO molecules and two tetraethylammonium counter-ions; b) 2D network established by cross-coordinated MC units, encapsulating tetraethylammonium in the interstices. Colour scheme: Cu - orange, O - red, N - blue, C - grey, H - white.

Table S1. Crystal data and structure refinement for **1** and **2**.

	1	**2**
Identification code	CCDC 1441662	CCDC 1441663
Empirical formula	C63 H53 Cu7 N15 O16	C53.36 H74.21 Cu5 N11.79 O14.21 S2.21
Formula weight	1720.98	1496.80
Temperature	85(2) K	85(2) K
Wavelength	1.54178 Å	1.54187 Å
Crystal system	Tetragonal	Monoclinic
Space group	P 4 21 2	P 21/c
Unit cell dimensions	a = 25.3614(6) Å	a = 15.9549(3) Å
a= 90°.		
	b = 25.3614(6) Å	b = 11.5822(2) Å
b= 90°.		
	c = 8.6031(6) Å	c = 16.8627(12) Å
g = 90°.		
Volume	5533.5(5) $Å^3$	3006.0(2) $Å^3$
Z	2	2
Density (calculated)	1.033 Mg/m^3	1.654 Mg/m^3
Absorption coefficient	1.859 mm^{-1}	3.296 mm^{-1}
F(000)	1734	1542
Crystal size	0.16 x 0.02 x 0.02 mm^3	0.100 x 0.100 x 0.020 mm^3
Theta range for data collection	3.897 to 68.209°.	6.651 to 68.249°.
Index ranges	-30<=h<=30, -30<=k<=30, -9<=l<=10	-19<=h<=19, -13<=k<=13, -20<=l<=20
Reflections collected	107642	80642
Independent reflections	5079 [R(int) = 0.2976]	5486 [R(int) = 0.0632]
Completeness to theta = 67.679°	99.7 %	99.9 %
Absorption correction	Semi-empirical from equivalents	Semi-empirical from equivalents
Max. and min. transmission	0.914 and 0.650	1.000 and 0.761
Refinement method	Full-matrix least-squares on F^2	Full-matrix least-squares on F^2
Data / restraints / parameters	5079 / 22 / 162	5486 / 24 / 446
Goodness-of-fit on F^2	1.008	1.042
Final R indices [I>2sigma(I)]	R1 = 0.1120, wR2 = 0.2727	R1 = 0.0605, wR2 = 0.1778
R indices (all data)	R1 = 0.1313, wR2 = 0.2917	R1 = 0.0647, wR2 = 0.1823
Absolute structure parameter	0.15(9)	n/a
Extinction coefficient	0.0095(13)	n/a
Largest diff. peak and hole	1.547 and -0.939 $e.Å^{-3}$	1.617 and -1.461 $e.Å^{-3}$

Table S2. Bond lengths [Å] for **1**.

O(11)-Cu(1)	1.890(10)
N(21)-Cu(3)	2.035(14)
O(31)-Cu(2)	1.919(8)
N(11)-Cu(1)	2.020(12)
Cu(3)-N(14)	1.93(2)
Cu(3)-O(15)	1.99(3)
Cu(2)-N(13)	2.322(3)
Cu(1)-N(12)	2.295(13)

Table S3. Bond lengths [Å] for **2**.

Cu(1)-O(11)	1.898(3)
Cu(1)-O(32)	1.918(3)
Cu(1)-N(11)	1.956(4)
Cu(1)-O(22)	1.979(3)
Cu(1)-N(14)	2.317(14)
Cu(1)-O(13)	2.366(5)
Cu(2)-O(12)	1.916(3)
Cu(2)-N(12)	1.937(4)
Cu(3)-O(32)	1.877(3)
Cu(3)-O(31)	1.899(3)

References:

1) CrystalStructure (Version 4.0), Single Crystal Structure Analysis Software. Rigaku Americas, 9009 TX, USA 77381-5209. Rigaku, Tokyo 196-8666, Japan.

2) G.M. Sheldrick, *Acta Cryst.*, 2008, **A64**, 112-122.

3a) A. Spek, *J. Appl. Cryst.*, 2003, **36**, 7-13; 3b) P. van der Sluis, A. L. Spek, *Acta Cryst.* 1990, **A46**, 194-201.

4) T. Haemers, J. Wiesner, D. Gießmann, T. Verbrugghen, U. Hillaert, R. Ortmann, H. Jomaa, A. Link, M. Schlitzer and S. Van Calenbergh, *Bioorg. Med. Chem.*, 2008, **16**, 3361-3371.